

## Optical Characteristics of Northern Safaga Bay Water and the Effect of Water Temperature and Salinity on it

Mahmoud El saman

National Institute of Oceanography and Fisheries, Cairo, Egypt.

mahmoud\_saman@yahoo.com

### ARTICLE INFO

#### Article History:

Received: Oct. 13, 2021

Accepted: April 5, 2022

Online: June 9, 2022

#### Keywords:

Red Sea,  
Safaga,  
Temperature,  
Salinity,  
Optical properties

### ABSTRACT

Compared to many world seas, the Red Sea is the warmest and the saltiest; it is characterized by low rainfall, no river flow and high evaporation rates. The optical characteristics of the seas and oceans are influenced by hydrological, biological and environmental conditions. Optical characteristics vary in the North of Safaga Bay due to the different hydrological conditions affecting the area. Temporal and spatial variations were detected in the incident solar radiation at the study site since each station is affected by different conditions. The impact of temperature and salinity on optical properties becomes clear upon applying the correlation between them. The average water temperature, water salinity, the intensity of the incident and irradiated flux intensity, transmittance, absorption and attenuation coefficient were 25.21°C, 42.10psu, 1420.26 w/m<sup>2</sup>, 74.84w/m<sup>2</sup>, 0.008, 0.92 and 0.85, respectively. Increased water temperature and low water salinity were associated with an increase in the intensity of radiation flow and frequent water transport. While, an increase in the absorption and dispersion factors were aligned with lower water temperature and higher salinity.

### INTRODUCTION

Solar radiation is of great importance in the marine environment, where solar energy drives the thermodynamics and photochemical processes in the sea, heating water, the movement of its layers, and its evaporation, in addition to the oxidation of marine pollutants. Moreover, it contributes to the initial production of the bottom by 90% or more in the total carbon fixation in some areas, where coral reefs spread in areas controlled by large cells (Delesalle *et al.* 1993; Borum & Jensen, 1996). Consequently, the link of optical properties measurements provided from satellites with the measurements of other ocean physics (e.g. wave properties, temperature, salinity, etc.) is more common with recent improved efforts in environmental monitoring (McCormick, 2006).

Seawater is a complex medium; transit solar radiation interacts with the ocean's water and the dissolved and suspended substances in it. The reaction takes the form of absorption and dispersion. The spectrum transmitted in sea water depends on the organic and inorganic substances dissolved in the water, and these components differ in concentrations with time and place since the sea is in permanent motion because of the surface winds, the tidal forces, and the rotation of the Earth, this makes it difficult to include the modeling of the diffusion of light in seawater (**Gupta, 1986; McCormick, 2006**). The optical and marine physical properties of coastal areas differ from those of the open areas in terms of time and location scales (**Chang & Dickey, 2001; Chang et al., 2002**) for the following reasons: 1) Fresh water entrance affecting fluid layers and their dynamics; 2) Suspended substances and pollutants present near the ocean surface and 3) There are more sources of particles from rivers.

The light scattering in the seawater has been theoretically and experimentally addressed. In the visible area (~ 400-700 nm), there is difficulty in measuring the absorption coefficient due to low absorption values in this region. Dissolved organics and suspended matter interfere with accurate measurements in the visible region (**Pegau, 1997**). The effect of temperature and salinity on the water absorption coefficient at the visible wavelengths has been studied both at laboratories and in fields. The absorption coefficient has been shown to depend on temperature and salinity at color tones of O - H tone frequencies in the infrared and semi-red part. **Trabjerg and Højerslevm (1996), Pegau (1997), Langford (2001), Sullivan et al. (2006)** and **Röttgers et al. (2010)** mentioned that the absorption coefficient of water depends on the temperature and salinity of sea water. This is attributed to the potential of the ions dissolved in seawater and temperature changes to change the structure of water molecule. The change in temperature and the concentration of ions changes the number of water molecules per volume by changing the density and partial density, respectively, thus changing the absorption coefficient as well. Recently, it was found that the absorption coefficient decreases with the increase in temperature (~ 0.001 m<sup>-1</sup>/°C) in the visible part of the spectrum (**Pegau & Zaneveld, 1993; Trabjerg & Højerslev, 1996**). The solar radiation in the Red Sea and its variability were addressed in the studies of **Acker et al. (2008), Brewin et al. (2013)** and **Brewin et al. (2015)**. Air bubbles in seawater caused by the breakage of waves in coastal areas are a major factor affecting the spread of light in water (**Zhang et al. 1998; Eric et al. 2001; Twardowski et al. 2012**). In addition, the atmospheric factors have a significant effect on the light attenuation factor in water (**Liu et al., 2014**).

The waters of the Red Sea are the warmest and the saltiest in the world (**Longhurst, 2007; Belkin, 2009; Raitzos et al., 2011, 2013**). They are characterized by low precipitation, no rivers flow (**Patzert, 1974**), and high evaporation rates (**Sofianos & Johns, 2003**). A variation is observed in the environmental conditions such as temperature, salinity, light intensity and nutrients in the Red Sea (**Sofianos & Johns,**

2003; Raitzos *et al.*, 2013; Churchill *et al.*, 2014; Sawall *et al.*, 2014; Ismael, 2015). The marine ecosystem of the Red Sea, including coral reefs, mangroves, and seaweed, is a suitable location for a wide variety of marine organisms (Belkin, 2009; Berumen *et al.*, 2013; Almahasheer *et al.*, 2016). It is considered undernourished due to a lack of nutrients in the surface layer (Raitzos *et al.* 2013, 2015; Triantafyllou *et al.*, 2014; Racault *et al.*, 2015). The optical characteristics can be affected by hydrological, biological and environmental conditions (Brewin *et al.*, 2015).

The ocean attenuation can be measured using various methods; the common method uses the Secchi disc, which is a weighed circular white disc with a diameter of 30cm. The Secchi disk slopes down into the seawater where it disappears from the sight; its reflection is equal to the intensity of the light diffused from the water. This depth in meters is divided into 1-7, resulting in attenuation, or the extinction of the light factor available as the mean depth of the Secchi disk. The light extinction coefficient ( $x$ ) can then be used in a form of Beer's law as follows:

$$I_z = I_0 e^{-xz}$$

Where,  $I_z$  is the light intensity at the depth  $z$ , and  $I_0$  is the light intensity on the ocean surface. This method gives no indication that the attenuation with depth has changed or that certain wavelengths of light have been attenuated.

This research aimed to identify the optical properties at four stations in Safaga Bay and determine the occurring differences and their causes and the effect of high water temperature and high salinity on the optical properties.

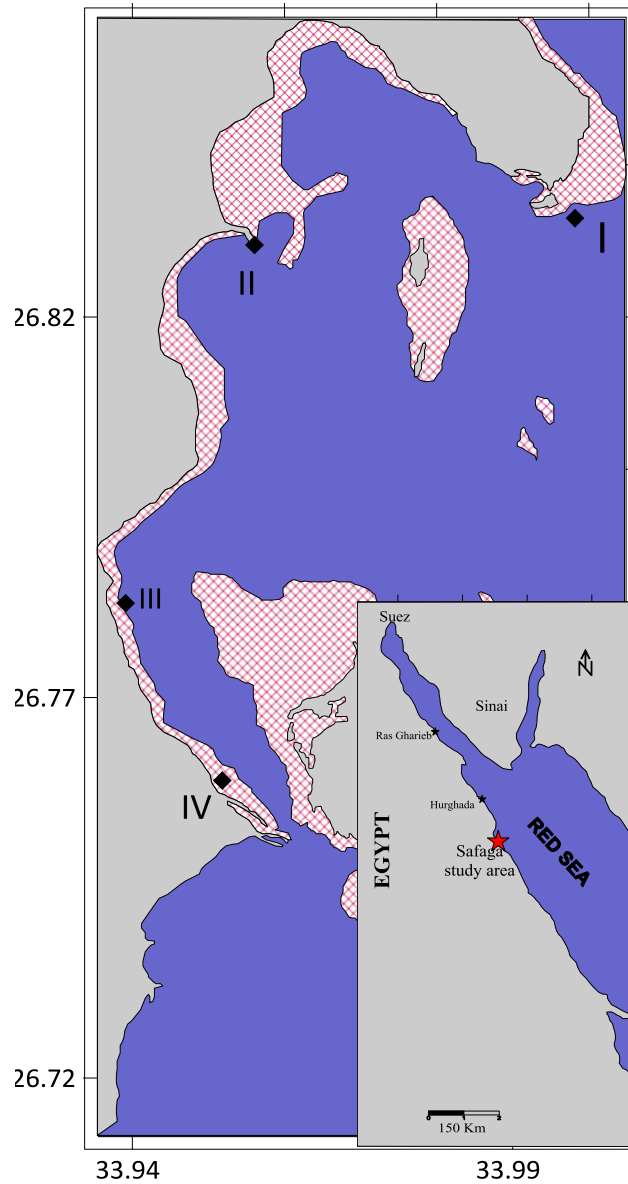
## **MATERIALS AND METHODS**

The northern Safaga Bay (NSB) is confined to latitudes  $26^{\circ} 37'$  &  $26^{\circ} 52'N$  and longitudes  $33^{\circ} 56'$  &  $34^{\circ} 00'$  (Fig. I). Four stations were chosen on the bay, with different locations (Table 1). Station I is affected by direct marine currents from the open sea that undergo the oceanographic characteristics of the sea, while station 2 is affected by marine currents of high temperature and salinity. For the third station, it is characterized by direct and heavily marine currents occurring in the event of fluctuations in water and increasing turbidity. High salinity currents flow and mix with currents flowing from the open sea, affecting the shallow fourth station that is used as a public beach. The mountain surrounds Safaga City from the southern west side.

The environmental data including temperature and salinity were seasonally examined near the bottom of every proceeding station, and they were recorded by Hydralb instrument (Surveyor<sup>(4)</sup>). While, the positions were determined by GPS (Magellan, 1000, 5000pro). Light intensity was collected by LI-189 Quantum/ Radiometer/ photometer, which records the intensity of the solar radiation falling in the air and the reflected beam. The map was plotted by golden software surfer 15.

**Table 1. Position of reference stations**

| areas       | Latitude (N)  | Longitude (E) |
|-------------|---------------|---------------|
| Station I   | 26° 50' 06.6" | 33° 59' 47.5" |
| Station II  | 26° 49' 45.6" | 33° 57' 21.8" |
| Station III | 26° 46' 07.9" | 33° 56' 32.1" |
| Station IV  | 26° 45' 29.8" | 33° 57' 04.3" |

**Fig. 1. Location map**

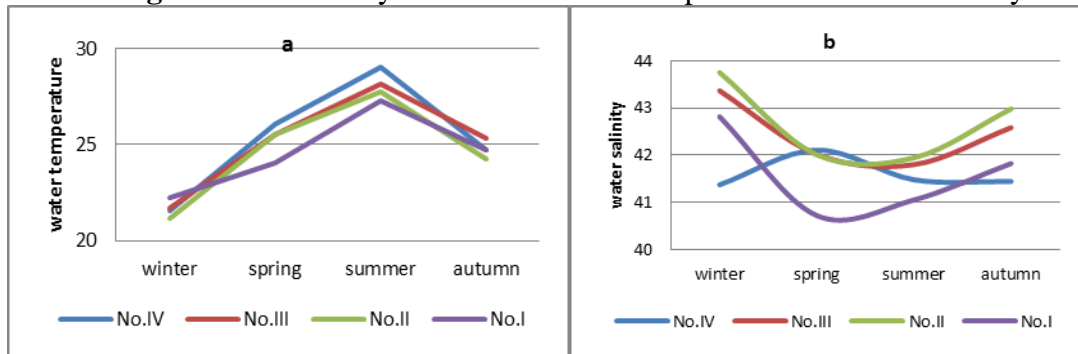
## RESULTS

### 1- Important physical properties

The low temperature values were recorded at the four stations during winter (Figure 2a), with average values of 22.2, 21.2, 21.7 and 21.6°C at I, II, III and IV stations, respectively. Temperatures reach their highest values during summer at the four stations as shown in the Fig. (2). Station IV recorded higher temperatures compared to the other three stations since it is affected by shallow water and streams flowing from the sea.

Salinity rises during winter and autumn and reaches its peak at Station II, while it decreases during summer and spring, reaching its lowest values in summer (Fig. 2b). Station II is located in shallow and semi-closed areas, thus the evaporation increases in this area, which subsequently increases salinity (Quail, 2014) as shown in Fig. (2b). Whereas, station I is affected by sea currents flowing from the sea; it has the same salinity level of the sea. The highest water salinity value (43.75psu) was recorded during winter at station II, while the lowest value (40.72 psu) was recorded during summer at station I.

**Fig.2.** The seasonally variation of water temperature and water salinity



### 2- Optical properties

The intensity solar radiation in the air records the lowest values during the winter, rises sharply to the highest values during the summer, and declines again during fall. The highest values were 1641.2, 1670, 1662.4 and 1683 w/m<sup>2</sup> (in spring), while the lowest values were 1036.7, 1130.2 (in autumn), 1001.2 and 1144.3 w/m<sup>2</sup> (in winter) at the stations I, II, III and IV, respectively. The southwestern mountains reflect solar radiation on the coast of the northern Safaga Gulf. This increases the intensity of solar radiation falling over the region, especially at the nearby station (Station IV), the recorded values of intensity solar radiation in the water of this station are higher than the rest of the station (Fig. 3c), while station I is far from the mountain effect, hence the values of the intensity of the penetrated solar radiation are moderate for the other part of the station. Notably, the intensity of irradiated fluxes of the four stations varies (Fig.3). Perpetually,

higher values were recorded at station I, compared to the other stations as a result of the high intensity of the solar radiation falling on the site and the lower values of temperature and salinity compared to the others. The intensity of irradiated fluxes at station I varies between 243 and 182.1w/m<sup>2</sup>. On the other hand, it is less intense with less variation at the other three stations, for instance at stations II and IV, the intensity of irradiated fluxes is very close, contrary to that recorded at station III. Water along with the melted sea salt is a very powerful infrared absorption agent (Woźniak & Dera, 2007). In contrast, visible light and ultraviolet radiation are heavily absorbed and dispersed by suspended organic matter from particles (Woźniak *et al.*, 2005a, 2005b, 2006). This includes the phytoplankton pigments (Woźniak *et al.* 2000a, 2000b; Woźniak & Dera, 2007).

In addition, the first station has a lower absorbent coefficient than the rest of the stations, ranging from 0.84 to 0.93 and the attenuation coefficient changes at a very small range (0.61 to 0.90), leading to a higher relative transmittance coefficient (0.07 to 0.16). The absorbent coefficient, attenuation coefficient and transmittance coefficient at stations II, III and IV is close, with averages of 0.92, 1.5 and 0.07.

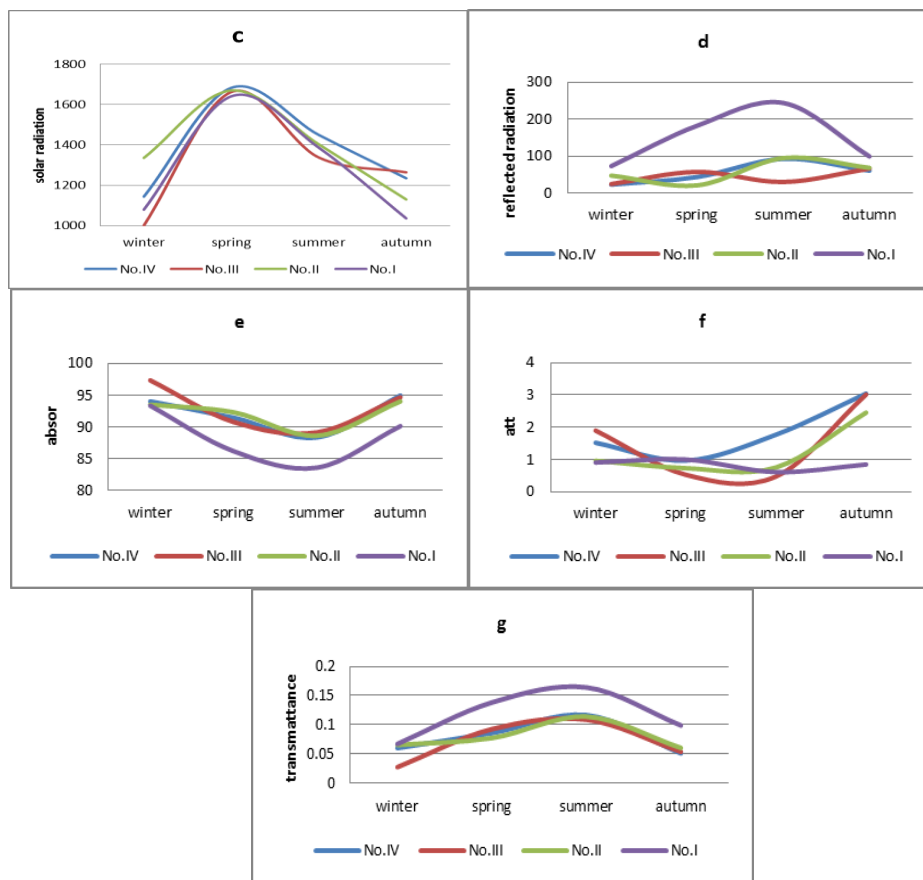


Fig. 3. The seasonally variations of optical components

## DISCUSSION

Water temperatures at the four study area vary, the highest of which was recorded at the 4<sup>th</sup> station during the study period, while the lowest was at the first station due to some topographic conditions. The first terminal is affected by offshore currents, while the second terminal is located in a shallow and semi-closed area. Station III is affected by a mixture of currents coming directly from the sea and currents coming from the shallow areas in the north of the Gulf as well. Furthermore, station IV is located in a shallow and semi-enclosed area and exposed to human pollution and sun radiation reflected from the nearing southwestern mountain.

**Table 2.** Correlation coefficient between temperature, salinity and optical components

| <i>Station</i> |             | irradiated<br>fluxes<br>intensity | absorption | attenuation | transmittance |
|----------------|-------------|-----------------------------------|------------|-------------|---------------|
| <i>I</i>       | temperature | 0.83                              | -0.86      | -0.82       | 0.86          |
|                | salinity    | -0.85                             | 0.91       | 0.14        | -0.91         |
| <i>II</i>      | temperature | 0.44                              | -0.81      | -0.21       | 0.81          |
|                | salinity    | -0.13                             | 0.72       | 0.36        | -0.72         |
| <i>III</i>     | temperature | 0.21                              | -0.91      | -0.46       | 0.91          |
|                | salinity    | -0.27                             | 0.98       | 0.65        | -0.98         |
| <i>IV</i>      | temperature | 0.9                               | -0.85      | -0.06       | 0.85          |
|                | salinity    | -0.13                             | -0.25      | -0.61       | 0.25          |

**Pegau *et al.* (1997)** reported that, the absorption coefficient of sea water depends on the water temperature in the near infrared position on the spectrum. By checking changes in water temperatures, irradiated fluxes intensity from the bottom, the absorption, transmittance and attenuation coefficients at the four stations under study. It can be concluded that water temperatures are directly proportional to irradiated fluxes intensity and transmittance coefficient except at the third station because the upwelling the water, while inversely proportional to both absorption and attenuation coefficients. It is noted that as water temperatures increase in the IV station, the irradiated fluxes intensity increases as shown by their correlation coefficient ( $R^2 = 0.90$ ), while absorption is reduced by the inverse relationship ( $R^2 = -0.85$ ) as in the table (2). Increasing the water temperatures at the same station also increase transmittance ( $R^2 = 0.85$ ) and an attenuation factor of as low as possible. The station I records the lowest water temperature values for the duration of the study, yet the temperature is directly proportional to the irradiated fluxes intensity ( $R^2=0.83$ ) and the transition factor ( $R^2=0.86$ ), while it is inverse proportional to the absorption coefficient ( $R^2=-0.86$ ) and the attenuation coefficient ( $R^2=-0.82$ ).

Water with the dissolved salts considered a very strong absorber of infrared radiation (**Woźniak and Dera, 2007**), while visible light and ultraviolet are scattering and absorbed from organic suspended matter (**Woźniak et al. 2005a, 2005b, 2006**). The salinity is directly proportional to the absorption coefficient of I, II and III stations and the correlation coefficient is up to  $R^2 = 0.91, 0.72$  and  $0.98$ , respectively. The water salinity is inversely proportional to the irradiated fluxes intensity and the transmittance to strong correlation coefficients as shown in the table (2).

It was clear that, when the water temperature up and water salinity drops, irradiated fluxes intensity and transmits become more frequent in the water, while lower water temperature and higher salinity, increase absorption and dispersion factors.

## CONCLUSION

The water temperature, salinity, intensity of incident and irradiated fluxes intensity were measured in four different stations in North Safaga bay. The transmittance, absorption and attenuation coefficient were calculated to find out the effect of temperature and salinity on the optical components. Therefore the average water temperature, water salinity, the intensity of the incident and irradiated fluxes intensity, transmittance, absorption and attenuation coefficient are  $25.21^\circ\text{C}$ ,  $42.10\text{psu}$ ,  $1420.26\text{ w/m}^2$ ,  $74.84\text{ w/m}^2$ ,  $0.008$ ,  $0.92$  and  $0.85$  respectively.

Water temperatures are directly proportional to irradiated fluxes intensity and transmittance coefficient, while inversely proportional to both absorption and attenuation coefficients. The salinity is directly proportional to the absorption coefficient and inversely proportional to the irradiated fluxes intensity and the transmittance. The optical inherent may be affected by the column water upwelling.

## REFERENCES

**Acker, J.; Leptoukh, G.; Shen, S.; Zhu, T. and Kempler, S.** (2008). Remotely-sensed chlorophyll a observations of the northern Red Sea indicate seasonal variability and influence of coastal reefs. *Journal of Marine Systems*, 69: 191–204.

**Almahasheer, H.; Aljowair, A.; Duarte, C. M. and Irigoien, X.** (2016). Decadal stability of Red Sea mangroves. *Estuarine Coastal and Shelf Sciences*, 169, 164–172.

**Belkin, I. M.** (2009). Rapid warming of large marine ecosystems. *Progress in Oceanography*, 81(1–4), 207–213.

**Berumen, M. L.; Hoey, A.; Bass, W.; Bouwmeester, J.; Catania, D. and Cochran, J. E.** (2013). The status of coral reef ecology research in the Red Sea. *Coral Reefs*, 32(3), 737–748.

**Borum, J. and Sand-Jensen, K.** (1996 ). Is total primary production in shallow coastal marine waters stimulated by nitrogen loading?, *Oikos*, 76, 406–410.

**Brewin, R.J.W.; Raitzos, D.E.; Pradhan, Y. and Hoteit, I.** (2013). Comparison of chlorophyll in the Red Sea derived from MODIS-Aqua and in vivo fluorescence. *Remote Sensing of Environment*, 136, 218–224.

**Brewin, R. J. W.; Raitzos, D. E.; Dall’Olmo, G.; Zarokanellos, N.; Jackson, T. and Racault, M.-F.** (2015). Regional ocean-colour chlorophyll algorithms for the Red Sea. *Remote Sensing Environment*, 165, 64–85.

**Chang, G. C. and Dickey T. D.** (2001), Optical and physical variability on timescales from minutes to the seasonal cycle on the New England Shelf: July 1996–June 1997, *J. Geophys. Res.*, 106, 9435– 9453.

**Chang, G. C.; Dickey, T. D.; Schofield, O. M.; Weidemann, A. D. ; Boss, E. ; Pegau, W. S.; Moline, M. A. and Glenn S. M.** (2002), Nearshore physical processes and bio-optical properties in the New York Bight, *J. Geophys Res.*, 107(C9).

**Churchill, J. H., Bower, A. S.; McCorkle, D. C. and Abualnaja, Y.** (2014). The transport of nutrient-rich Indian Ocean water through the Red Sea and into coastal reef systems. *Journal of Marine Research*, 72(3):165–181.

**Delesalle, B.; Pichon, M.; Frankignoulle, M. and Gattuso, J.** (1993). Effects of a cyclone on coral reef phytoplankton biomass, primary production and composition (Moorea island, French Polynesia), *J. Plankton Res.*, 15, 1413–1423.

**Eric J.; Terrill, W.; Melville, K. and Stramski, D.** (2001). Bubble entrainment by breaking waves and their influence on optical scattering in upper ocean”, *J. Geophys. Res.*, 106(C8), 16815-16823

**Gupta s, K.** (1986). Spectral Transmission Studies of Ocean Water under Different Sea. *DcfSci J*, Vol 34, pp 19-28.

**Ismael, A. A.** (2015). Phytoplankton of the Red Sea. In *The Red Sea*. Berlin, Germany: Springer pp. 567–583.

**Langford, V. S.; McKinley, A. J. and Quickenden T. I.** (2001). Temperature dependence of the visible-near-infrared absorption spectrum of liquid water. *J. Phys. Chem. A* 105: 8916-8921.

**Liu, J.; Shi, J.; Tang, Y.; Zhu, K.; Ge, Y.; Chen, X.; He, X. and Liu, D.** (2014). Effect of atmospheric environment on the attenuation coefficient of light in Water. arXiv, Dahe Liu dhliu@bnu.edu.cn

**Longhurst, A.** (2007). Toward an ecological geography of the sea. In *Ecological geography of the sea* (pp. 1–17). Amsterdam, the Netherlands.

**McCormick N. J.**, (2006). *Transport Theory for Optical Oceanography* University of Washington, Mechanical Engineering Department, Seattle, Washington 98195-2600.

**Patzert, W. C.** (1974). Wind-induced reversal in Red Sea circulation. *Deep Sea Research and Oceanographic Abstracts*, 21(2), 109–121.

**Pegau, W. S. and Zaneveld, J. R. V.** (1993). Temperature-dependent absorption of water in the red and near-infrared portions of the spectrum,” *Limnol. Oceanogr.* 38, 188–192 .

**Pegau, W. S.; D. Gray, and Zaneveld, V.** (1997). Absorption and attenuation of visible and near-infrared light in water: dependence on temperature and salinity. *Applied Optics* Vol. 36, No. 24 .

**Racault, M.F.; Raitzos, D. E.; Berumen, M. L.; Brewin, R. J. W. ; Platt, T. and Sathyendranath, S.** (2015). Phytoplankton phenology indices in coral reef ecosystems: Application to ocean-color observations in the Red Sea. *Remote Sensing Environment*, 160, 222–234.

**Raitzos, D. E.; Hoteit, I.; Prihartato, P. K.; Chronis, T.; Triantafyllou, G and Abualnaja, Y.** (2011). Abrupt warming of the Red Sea. *Geophysical Research Letters*, 38, L14601. <https://doi.org/10.1029/2011GL047984>

**Raitzos, D. E.; Pradhan, Y.; Brewin, R. J. W.; Stenchikov, G. and Hoteit, I.** (2013). Remote sensing the phytoplankton seasonal succession of the Red Sea. *Plos One*, 8(6), e64909.

**Raitzos, D. E.; Yi, X.; Platt, T.; Racault, M.-F.; Brewin, R. J. W. and Pradhan, Y.** (2015). Monsoon oscillations regulate fertility of the Red Sea. *Geophysical Research Letters*, 42, 855–862.

**Röttgers, R.; Doerfer, R.; McKee, D. and Schönfeld, W.** (2010). The Water Optical Properties Processor (WOPP): Pure water spectral absorption, scattering, and real part of refractive index model, Algorithm Technical Basis Document, report number, WR D6.

**Sawall, Y.; Al-Sofyani, A.; Banguera-Hinestroza, E. and Voolstra, C. R.** (2014). Spatio-Temporal Analyses of Symbiodinium Physiology of the Coral *Pocillopora verrucosa* along Large-Scale Nutrient and Temperature Gradients in the Red Sea. *PLoS ONE* 9(8) e103179

**Sofianos, S. S. and Johns, W. E.** (2003). An Oceanic General Circulation Model (OGCM) investigation of the Red Sea circulation: 2. Threedimensional circulation in the Red Sea. *Journal of Geophysical Research*, 108(C3), 2002.

**Sullivan, J. M.; Twardowski, M. S.; Zaneveld, J. R. V.; Moore, C. M.; Barnard, A. H.; Donaghay, P. L. and Rhoades, B.** (2006). The hyperspectral temperature and salt dependencies of absorption by water and heavy water in the 400–750 nm spectral range. *Appl. Opt.* 45:5294-53090.

**Trabjerg and Højerslev, N. K.** (1996). Temperature influence on light absorption by fresh water and seawater in the visible and near-infrared spectrum,” *Appl. Opt.* 35, 2653–2658.

**Triantafyllou, G.; Yao, F.; Petihakis, G.; Tsiaras, K. P.; Raitzos, D. E. and Hoteit, I.** (2014). Exploring the Red Sea seasonal ecosystem functioning using a three-dimensional biophysical model. *Journal of Geophysical Research: Oceans*, 119, 1791–1811.

**Twardowski M., X.; Zhang, S.; Vagle, J.; Sullivan, S.; Freeman, H.; Czerski, Y.; You, L.; Bi and Kattawar, G.** (2012). The optical volume scattering function in a surf zone inverted to derive sediment and bubble particle subpopulations”, *J. Geophys. Res.*, 117, C00H17

**Zhang, X.; Lewis, M. and Johnson B.** (1998). Influence of bubbles on scattering of light in the ocean”, *Appl. Opt.*, 37, 6225-6536

**Woźniak B.; Woźniak, S.B.; Tyszka, K.; Ostrowska, M.; Ficek, D.; Majchrowski, R. and Dera, J.** (2006), Modelling the light absorption properties of particulate matter forming organic particles suspended in seawater. Part 3. Practical application, *Oceanologia*, 48 (4), 479–507.

**Woźniak, B. and Dera, J.** (2007). *Light absorption in sea water*, Springer, New York, 452 pp.

**Woźniak, B.; Dera, J.; Ficek, D.; Majchrowski, R.; Kaczmarek, S.; Ostrowska, M. and Koblentz-Mishke, O. I.** (2000a). Model of ‘in vivo’ spectral absorption of algal pigments, *Ocean Optics XV Conf. [CD ROM]*, 1062, Off. Naval Res. Ocean, Atmos. Space S&T Dept., 11.

**Woźniak, B.; Dera, J.; Ficek, D.; Majchrowski, R.; Kaczmarek, S.; Ostrowska, M. and Koblenz-Mishke, O. I.** (2000b). Model of the 'in vivo' spectral absorption of algal pigments. Part 1. Mathematical apparatus, *Oceanologia*, 42 (2), 177–190.

**Woźniak, B.; Woźniak, S.B.; Tyszka, K.; Ostrowska, M.; Majchrowski, R.; Ficek, D. and Dera, J.**; (2005b). Modelling the light absorption properties of particulate matter forming organic particles suspended in seawater. Part 2. Modelling results, *Oceanologia*, 47 (4), 621–662.

**Woźniak, B.; Woźniak, S.B.; Tyszka, K. and Dera, J.** (2005a). Modelling the light absorption properties of particulate matter forming organic particles suspended in seawater. Part 1. Model description, classification of organic particles, and example spectra of the light absorption coefficient and the imaginary part of the refractive index of particulate matter for phytoplankton cells and phytoplankton-like particles, *Oceanologia*, 47 (2), 129–164.